

# A TURN-OVER SCENARIO FOR ROTATING MAGNETIC WHITE DWARFS: MODELS WITH SEVERAL VALUES OF MASS, ANGULAR MOMENTUM, AND MAGNETIC FIELD

V. S. Geroyannis and P. J. Papasotiriou

*Astronomy Laboratory, Department of Physics, University of Patras, Greece,*

*GR-26500 PATRAS, GREECE*

[vgeroyan@physics.upatras.gr](mailto:vgeroyan@physics.upatras.gr), [papasot@physics.upatras.gr](mailto:papasot@physics.upatras.gr)

## ABSTRACT

We study a white dwarf model with differential rotation and magnetic field, for which the symmetry axis of the toroidal field, the magnetic axis of the poloidal field, and the principal axis  $I_3$  coincide permanently; the common axis defined this way is called “magnetic symmetry axis”. Furthermore, the magnetic symmetry axis inclines at a small angle  $\chi$  relative to the spin axis of the model; this angle is called “obliquity angle” or “turn-over angle”. Such a model is almost axisymmetric and undergoes an early evolutionary phase of secular timescale, characterized by the fact that the moment of inertia along the spin axis,  $I_{zz} \simeq I_{33}$ , is greater than the moments of inertia along the (almost) equatorial axes,  $I_{11} = I_{22}$ , since rotation and poloidal field (both responsible for the oblateness of the model) dominate over the toroidal field (responsible, in turn, for the prolateness of the model). During this early evolutionary phase, the model suffers from secular angular momentum loss due to weak magnetic dipole radiation activated by the poloidal field. Such an angular momentum loss leads gradually to a situation of dynamical asymmetry with  $I_{11} > I_{33}$ . However, dynamically asymmetric configurations tend to turn over spontaneously, that is, to rotate about axis with moment of inertia greater than  $I_{33}$  with angular momentum remaining invariant. So, the fate of a dynamically asymmetric configuration is to become an oblique rotator and, eventually, a perpendicular rotator. During the so-called “turn-over phase”, the turn over angle,  $\chi$ , increases spontaneously up to  $\sim 90^\circ$  on a “turn-over timescale”,  $t_{\text{TOV}}$ , since the rotational kinetic energy of the model decreases from a higher level when  $\chi \simeq 0^\circ$  (aligned rotator) to a lower level when  $\chi \simeq 90^\circ$  (perpendicular rotator). At this lower level the model reaches the state of least energy consistent with its prescribed angular momentum and magnetic field. The excess rotational kinetic energy due to differential rotation is totally dissipated due to the action of turbulent viscosity in the convective regions of the model. In the present paper, we study numerically the so-called “turn-over scenario” (i.e., an evolutionary scenario, which takes into account the turn-over phase) for white dwarf models of several masses, angular momenta, and magnetic fields.

*Subject headings:* stars: magnetic fields — stars: rotation — white dwarfs

## 1. Introduction

In a recent paper (Geroyannis 2001, hereafter Paper I, and references therein), the turn-over scenario has been studied numerically for rotating magnetic white dwarfs (see also Geroyannis 2002). The turn-over scenario, hereafter TOV scenario, deals with the problem of rotational evolution of a star by taking into account the gradual increase of the turn-over angle, i.e., the angle between the magnetic symmetry axis and the spin axis of the star.

In the TOV scenario, we assume that the differentially rotating white dwarf model is initially almost axisymmetric (i.e., its turn-over angle  $\chi$  is small:  $\chi \leq 2^\circ$ , say) and undergoes an “early evolutionary phase”, during which rotation and poloidal field prevail against the toroidal field, yielding oblate configurations with  $I_{33} > I_{11}$  (where  $I_{33}$  is the moment of inertia along the magnetic symmetry axis, almost coinciding with the spin axis, and  $I_{11} = I_{22}$  are the moments of inertia along the other two principal axes).

However, due to a weak magnetic dipole radiation activated by the poloidal field, the toroidal field becomes gradually more effective, and eventually leads the model to the so-called “late evolutionary phase”, during which the model suffers from “dynamical asymmetry”:  $I_{11} > I_{33}$ .

Dynamical asymmetry leads the model to the so-called “turn-over phase”, during which the turn-over angle,  $\chi$ , increases spontaneously up to  $\sim 90^\circ$  on a turn-over timescale,  $t_{\text{TOV}}$ . The terminal model rotates about its  $I_1$  axis, coinciding with the invariant angular momentum axis, and occupies the state of least energy consistent with its angular momentum and magnetic field. The excess energy due to differential rotation, defined by the angular velocity component  $\Omega_3$  along the spontaneously turning over  $I_3$  axis (permanently coinciding with the magnetic symmetry axis), is dissipated down to zero due to the efficient action of turbulent viscosity in the convective zone of the model. So, the terminal model does not rotate about its magnetic symmetry axis. Furthermore, it seems difficult for the terminal model to sustain differential rotation along its  $I_1$  axis, mainly due to the destructive action of the poloidal field. In particular, there is a competition between the efforts of the magnetic stresses to remove rotational nonuniformities, and those of the rotational velocities to bury and destroy the magnetic flux. If the magnetic field and the electrical conductivity have appropriate values (see especially § 7 of Paper I), then the magnetic field prevails and removes all the nonuniformities of rotation. So, the terminal model rotates rigidly about its  $I_1$  principal axis with angular velocity  $\Omega_1$ .

In Paper I, the aim was to compute the so-called “optimal values” for the angular momentum,  $L_{xx}$ , the average surface poloidal field,  $B_s$ , and the time evolution parameter,  $\delta$ , under which the model starts its turn-over phase (Paper I, § 6). In the present paper, on the other hand, our aim is slightly different. In particular, we shall study several possible turn-over scenarios, corresponding to several indicative values  $L_{xx}$  and  $B_s$ . We shall describe in detail our computations in the following

sections.

## 2. The model, the numerical method, and the computations

We shall use hereafter definitions and symbols identical to those in Paper I.

The model and the numerical method used in the study of the TOV scenario have been thoroughly discussed in Paper I. All the technical details of that paper are closely related to each other in a way making difficult to summarize some issues without summarizing the remaining issues of the whole matter. Since our intention is to avoid repeating that paper here, we clearly consider the present paper as continuation of Paper I.

For the computations of the present paper, we assume that the angular momentum,  $L_{xx}$ , and the average surface poloidal field,  $B_s$ , of the starting model are free model parameters (in Paper I, instead, we have computed optimal values for these quantities; see especially § 6 of that paper). Accordingly, the spin-down time rate due to turn-over,  $\dot{P}_{\text{TOV}}$ , becomes now a dependent model parameter taking several values for several choices of the whole set of the free model parameters.

We study the TOV scenario for three “reference” cases of white dwarfs; namely, (a)  $M = M_{\text{REF1}} = 0.6 M_\odot$  and  $P = P_{\text{REF1}} = 142 \text{ s}$ , (b)  $M = M_{\text{REF2}} = 0.9 M_\odot$  and  $P = P_{\text{REF2}} = 33 \text{ s}$ , (c)  $M = M_{\text{REF3}} = 1.32 M_\odot$  and  $P = P_{\text{REF3}} = 8 \text{ s}$ . For all these cases, we assume a “reference” period time rate,  $|\dot{P}_{\text{REF}}| = 5 \times 10^{-13} \text{ ss}^{-1}$ , which should be dominant in the absence of the spin-down time rate due to turn-over,  $\dot{P}_{\text{TOV}}$ . Our purpose is to study the variation of the ratio  $\dot{P}_{\text{TOV}}/|\dot{P}_{\text{REF}}|$  with the free parameters  $L_{xx}$  and  $B_s$ , and to find when  $\dot{P}_{\text{TOV}}$  becomes of comparable or even higher significance with respect to  $\dot{P}_{\text{REF}}$  (the latter could be due to accretional activity around the star and its actual sign — spin-down for plus, spin-up for minus — is insignificant here). All the starting models are assumed to be in a state of “physical differential rotation”,  $F_r = 1$ .

For each case, we consider seven “representative” values for (a) the angular momentum,  $L_{xx}$ , and (b) the average surface poloidal field,  $B_s$ . The lower value of angular momentum adopted corresponds to a turn-over phase just started, while the higher angular momentum adopted corresponds to a turn-over phase near its end.

The turn-over phase can be easily understood in a graph showing the period as a function of angular momentum,  $P(L)$ , for both the aligned and perpendicular rotators (Fig. 1). The angular momentum remains constant during the turn-over. Consequently, a turn-over phase is shown in the  $P(L)$  graph as a vertical arrow, connecting the starting model (located at the aligned rotator’s curve) with the terminal model (located, in turn, at the perpendicular rotator’s curve).

### 3. Results and discussion

Computed parameters for the aligned and the perpendicular rotators are given in Tables 1–14. In Tables 1, 6, and 11, we give parameters regarding the aligned rotators. These parameters are almost independent of the average surface poloidal field,  $B_s$ ; namely, the central period,  $P_{xx}$ , the rotational kinetic energy,  $T_{xx}$ , the moments of inertia  $I_{11}$  and  $I_{33}$  along the principal axes  $I_1$  and  $I_3$ , the average surface toroidal field,  $\langle H_{ts} \rangle$ , the maximum toroidal field,  $H_{t[\max]}$ , the average toroidal field,  $\langle H_t \rangle$ , and the ratio  $\omega_e^{-1} = \Omega_c/\Omega_e$ , where  $\Omega_c$ ,  $\Omega_e$  are the central and equatorial angular velocities, respectively. The corresponding parameters for the perpendicular rotators are given in Tables 3, 8, and 13. Here,  $P_{RR}$  is the central period and  $T_{RR}$  is the rotational kinetic energy of the perpendicular rotator.

Parameters regarding the aligned rotators and varying with the average surface poloidal field,  $B_s$ , are given in Tables 2, 7, and 12; namely, the corresponding poloidal magnetic parameter,  $\beta_*^p$ , the surface Alfvén speed,  $V_{As}$ , the surface Alfvén time,  $t_{As}$ , the maximum poloidal field,  $H_{p[\max]}$ , and the average poloidal field,  $\langle H_p \rangle$ . The corresponding parameters for the perpendicular rotators are given in Tables 4, 9, and 14.

General results concerning the turn-over phase are given in Tables 5, 10, and 15. Parameters tabulated in these tables are the magnetic flux,  $f$ , the turn-over timescale,  $t_{TOV}$ , the spin-down time rate due to turn-over,  $\dot{P}_{TOV}$ , the turn-over timescale in units of the starting central period,  $N_{xx} = t_{TOV}/P_{xx}$ , the present turn-over time,  $t_{now}$ , and the power loss due to turn-over,  $\dot{T}$ . These tables also contain three parameters which are independent of the average surface poloidal field; namely, the rigid rotation amplification ratio,  $A_r$ , the current turn-over angle,  $\chi_{now}$ , and the current differential rotation strength,  $F_{r[now]}$ .

Our numerical results reveal that the turn-over timescale,  $t_{TOV}$ , varies from  $\sim 0.4$  to  $\sim 7300$  million years, dependent on the mass of the model, the angular momentum, and the average surface poloidal field of the starting model. The turn-over angles  $\chi_{now}$ , corresponding to the present turn-over times  $t_{now}$ , vary from  $\sim 3^\circ$  to  $\sim 90^\circ$ .

An issue of particular interest is the estimated values for the spin-down time rate due to turn-over,  $\dot{P}_{TOV}$ , which vary from  $4.3 \times 10^{-17} \text{ ss}^{-1}$  to  $1.1 \times 10^{-12} \text{ ss}^{-1}$ . From columns 1 and 4 of Tables 5, 10, and 15, it is apparent that, for low values of the surface poloidal field, the turn-over spin-down is negligible, since  $\dot{P}_{TOV} \ll |P_{REF}|$ . However, high values of the surface poloidal field lead to values of  $\dot{P}_{TOV}$  which are comparable to or even greater than  $|P_{REF}|$  (Figs. 2, 3, and 4). For such high values of  $B_s$ ,  $\dot{P}_{TOV}/|P_{REF}|$  depends only weakly on the particular values of  $L_{xx}$  (roughly speaking, it is independent of  $L_{xx}$ ). Consequently, in a white dwarf which is now in its turn-over phase, the turn-over effects are negligible if the surface poloidal field is weak; on the other hand, if the surface poloidal field is strong or even moderate, the turn-over effects to the time rate of the central period cannot be neglected.

## ACKNOWLEDGMENTS

The research reported here was supported by the Research Committee of the University of Patras (C. Carathéodory's Research Project 1998/1932).

## REFERENCES

- Geroyannis, V. S. 2001, astro-ph/0103080 (Paper I)  
Geroyannis, V. S. 2002, ApJS, to appear in Vol. 141 No. 2

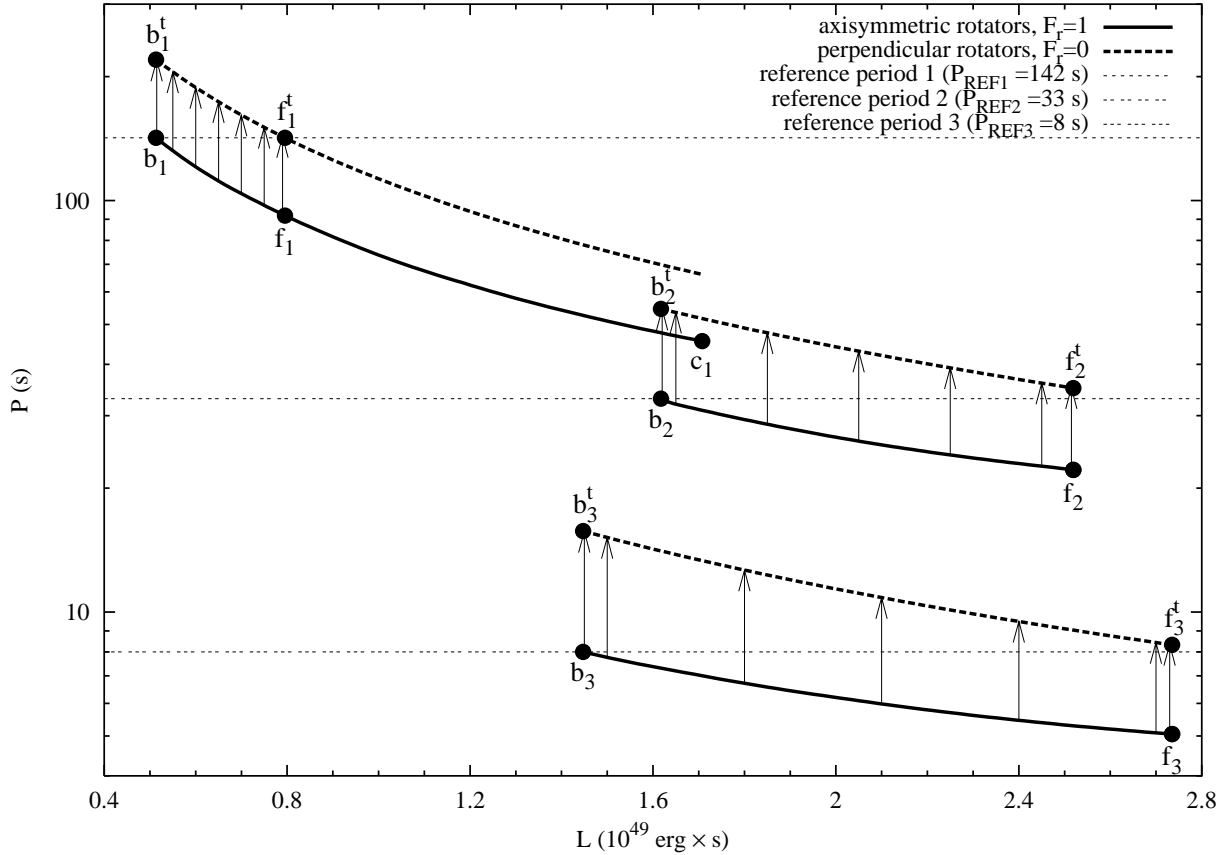


Fig. 1.— Plot of period at center,  $P$ , as a function of angular momentum,  $L$ , for both the aligned rotators (thick solid curves) and the perpendicular rotators (thick dashed curves). Points  $b_1, b_2, b_3$ : models with central periods equal to the “reference” periods studied in this paper,  $P_{\text{REF}1} = 142 \text{ s}$ ,  $P_{\text{REF}2} = 33 \text{ s}$ ,  $P_{\text{REF}3} = 8 \text{ s}$ ; points  $b_1^t, b_2^t, b_3^t$ : terminal models corresponding to the starting models  $b_1, b_2, b_3$ ; points  $f_1, f_2, f_3$ : starting models with maximum possible angular momentum; points  $f_1^t, f_2^t, f_3^t$ : terminal models corresponding to the starting models  $f_1, f_2, f_3$ ; point  $c_1$ : model for which  $I_{33} = I_{11} = I_{22}$  (note that corresponding models for the second and third case,  $c_2, c_3$ , coincide with the points  $f_2, f_3$ , respectively). Vertical arrows show possible turn-over scenarios currently in progress, which are studied numerically in this paper.

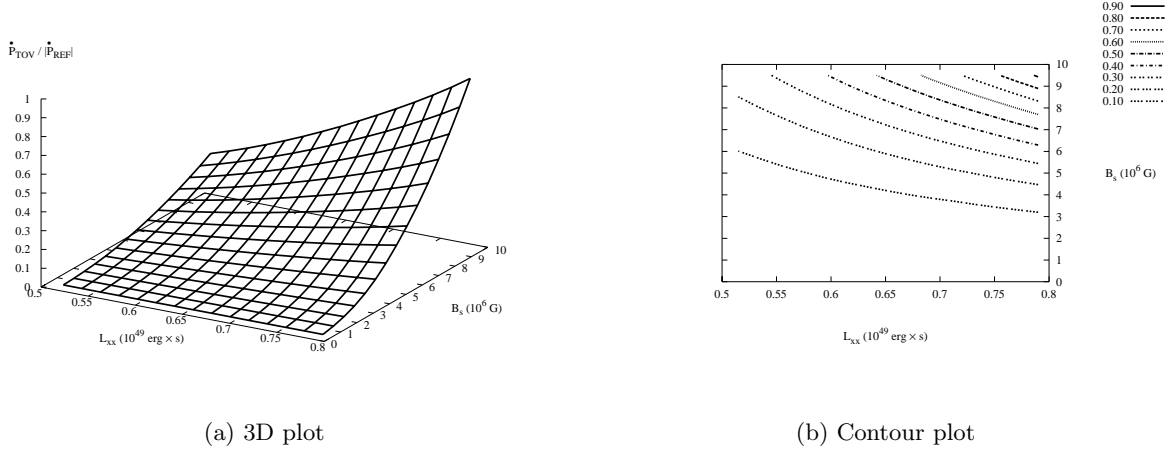


Fig. 2.— The ratio  $(dP_{\text{TOV}1}/dt) / |dP_{\text{REF}1}/dt|$  as a function of  $L_{xx}$  and  $B_s$  for the case  $M = 0.6 M_\odot$ .

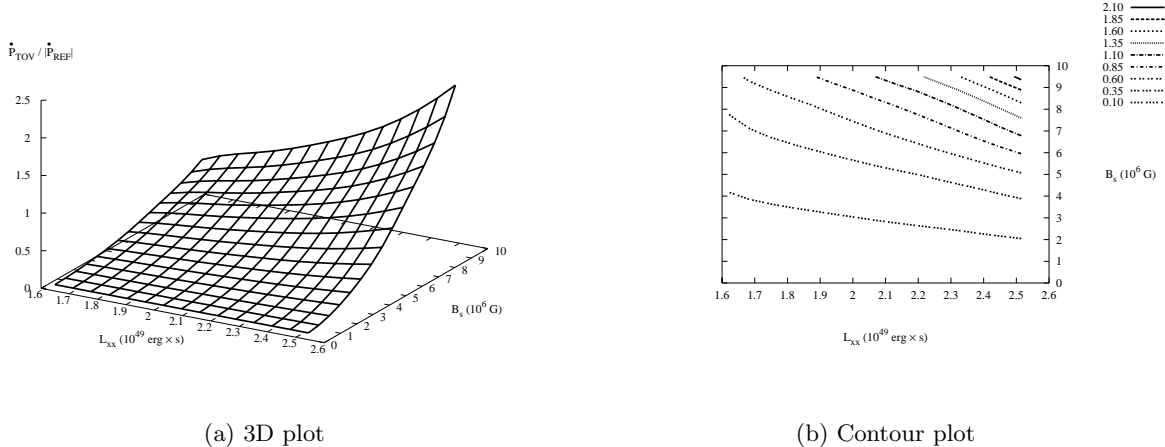


Fig. 3.— The ratio  $(dP_{\text{TOV}2}/dt) / |dP_{\text{REF}2}/dt|$  as a function of  $L_{xx}$  and  $B_s$  for the case  $M = 0.9 M_\odot$ .

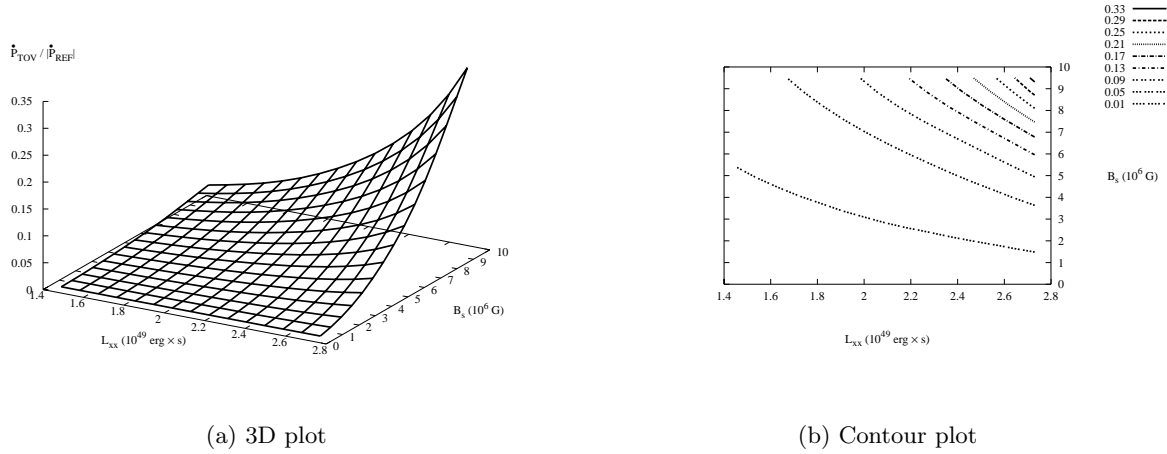


Fig. 4.— The ratio  $(dP_{\text{TOV3}}/dt) / |dP_{\text{REF3}}/dt|$  as a function of  $L_{xx}$  and  $B_s$  for the case  $M = 1.32 M_\odot$ .

Table 1. Case  $M/M_{\odot} = 0.6$ : Results concerning the aligned rotator (part I)

$L_{xx}$	$P_{xx}$	$T_{xx}$	$I_{11}$	$I_{33}$	$\langle H_{ts} \rangle$	$H_{t[\max]}$	$\langle H_t \rangle$	$\omega_e^{-1}$
5.150e+48	141.5427	8.0177e+46	1.7858e+50	1.7336e+50	4.3306e+09	2.6760e+11	1.1623e+11	3.2106
5.500e+48	132.1198	9.1358e+46	1.7868e+50	1.7353e+50	4.3314e+09	2.6739e+11	1.1613e+11	3.2105
6.000e+48	120.7721	1.0856e+47	1.7884e+50	1.7380e+50	4.3326e+09	2.6706e+11	1.1600e+11	3.2105
6.500e+48	111.5137	1.2719e+47	1.7900e+50	1.7409e+50	4.3339e+09	2.6670e+11	1.1585e+11	3.2104
7.000e+48	103.9030	1.4725e+47	1.7918e+50	1.7440e+50	4.3353e+09	2.6632e+11	1.1569e+11	3.2091
7.500e+48	97.3565	1.6870e+47	1.7938e+50	1.7474e+50	4.3367e+09	2.6591e+11	1.1552e+11	3.2091
7.900e+48	92.5301	1.8687e+47	1.7954e+50	1.7503e+50	4.3380e+09	2.6556e+11	1.1537e+11	3.2090

Note. — In all tables, parameters are given in cgs units, unless stated otherwise.

Table 2. Case  $M/M_{\odot} = 0.6$ : Results concerning the aligned rotator (part II)

$B_s$	$\beta_*^p$	$V_{As}$	$t_{As}$	$H_p[\max]$	$\langle H_p \rangle$
Models with $L_{xx} = 5.150e+48$					
5.0e+05	7.7169e+04	1.1829e+03	7.3680e+05	9.8731e+06	3.4973e+06
2.0e+06	1.9291e+04	4.7319e+03	1.8419e+05	3.9494e+07	1.3990e+07
3.5e+06	1.1025e+04	8.2798e+03	1.0527e+05	6.9107e+07	2.4479e+07
5.0e+06	7.7170e+03	1.1829e+04	7.3681e+04	9.8731e+07	3.4972e+07
6.5e+06	5.9363e+03	1.5377e+04	5.6679e+04	1.2835e+08	4.5463e+07
8.0e+06	4.8225e+03	1.8929e+04	4.6044e+04	1.5799e+08	5.5963e+07
9.5e+06	4.0606e+03	2.2481e+04	3.8770e+04	1.8763e+08	6.6463e+07
Models with $L_{xx} = 5.500e+48$					
5.0e+05	7.7143e+04	1.1829e+03	7.3695e+05	9.8679e+06	3.4956e+06
2.0e+06	1.9286e+04	4.7317e+03	1.8424e+05	3.9471e+07	1.3982e+07
3.5e+06	1.1021e+04	8.2798e+03	1.0529e+05	6.9070e+07	2.4467e+07
5.0e+06	7.7151e+03	1.1828e+04	7.3703e+04	9.8668e+07	3.4952e+07
6.5e+06	5.9345e+03	1.5377e+04	5.6692e+04	1.2827e+08	4.5440e+07
8.0e+06	4.8206e+03	1.8930e+04	4.6051e+04	1.5791e+08	5.5940e+07
9.5e+06	4.0606e+03	2.2473e+04	3.8791e+04	1.8747e+08	6.6409e+07
Models with $L_{xx} = 6.000e+48$					
5.0e+05	7.7104e+04	1.1829e+03	7.3719e+05	9.8597e+06	3.4931e+06
2.0e+06	1.9277e+04	4.7316e+03	1.8430e+05	3.9438e+07	1.3972e+07
3.5e+06	1.1016e+04	8.2798e+03	1.0532e+05	6.9012e+07	2.4450e+07
5.0e+06	7.7096e+03	1.1831e+04	7.3711e+04	9.8608e+07	3.4935e+07
6.5e+06	5.9307e+03	1.5379e+04	5.6703e+04	1.2818e+08	4.5413e+07
8.0e+06	4.8187e+03	1.8928e+04	4.6072e+04	1.5776e+08	5.5892e+07
9.5e+06	4.0588e+03	2.2472e+04	3.8806e+04	1.8730e+08	6.6357e+07
Models with $L_{xx} = 6.500e+48$					
5.0e+05	7.7061e+04	1.1829e+03	7.3744e+05	9.8508e+06	3.4903e+06
2.0e+06	1.9265e+04	4.7317e+03	1.8436e+05	3.9403e+07	1.3961e+07
3.5e+06	1.1008e+04	8.2808e+03	1.0534e+05	6.8959e+07	2.4433e+07
5.0e+06	7.7058e+03	1.1830e+04	7.3741e+04	9.8512e+07	3.4905e+07
6.5e+06	5.9270e+03	1.5380e+04	5.6719e+04	1.2808e+08	4.5380e+07
8.0e+06	4.8169e+03	1.8925e+04	4.6095e+04	1.5760e+08	5.5839e+07
9.5e+06	4.0550e+03	2.2480e+04	3.8805e+04	1.8720e+08	6.6329e+07
Models with $L_{xx} = 7.000e+48$					
5.0e+05	7.7015e+04	1.1829e+03	7.3771e+05	9.8415e+06	3.4874e+06
2.0e+06	1.9254e+04	4.7316e+03	1.8443e+05	3.9365e+07	1.3949e+07
3.5e+06	1.1003e+04	8.2800e+03	1.0539e+05	6.8886e+07	2.4411e+07
5.0e+06	7.7021e+03	1.1828e+04	7.3777e+04	9.8407e+07	3.4871e+07
6.5e+06	5.9233e+03	1.5380e+04	5.6738e+04	1.2796e+08	4.5343e+07

Table 2—Continued

$B_s$	$\beta_*^p$	$V_{As}$	$t_{As}$	$H_p[\max]$	$\langle H_p \rangle$
8.0e+06	4.8131e+03	1.8928e+04	4.6104e+04	1.5747e+08	5.5802e+07
9.5e+06	4.0532e+03	2.2477e+04	3.8825e+04	1.8700e+08	6.6264e+07
Models with $L_{xx} = 7.500\text{e+48}$					
5.0e+05	7.6965e+04	1.1829e+03	7.3800e+05	9.8314e+06	3.4843e+06
2.0e+06	1.9241e+04	4.7317e+03	1.8450e+05	3.9326e+07	1.3937e+07
3.5e+06	1.0995e+04	8.2803e+03	1.0543e+05	6.8819e+07	2.4390e+07
5.0e+06	7.6965e+03	1.1829e+04	7.3799e+04	9.8315e+07	3.4843e+07
6.5e+06	5.9196e+03	1.5380e+04	5.6761e+04	1.2783e+08	4.5302e+07
8.0e+06	4.8094e+03	1.8930e+04	4.6116e+04	1.5733e+08	5.5759e+07
9.5e+06	4.0513e+03	2.2473e+04	3.8847e+04	1.8677e+08	6.6193e+07
Models with $L_{xx} = 7.900\text{e+48}$					
5.0e+05	7.6924e+04	1.1829e+03	7.3824e+05	9.8230e+06	3.4817e+06
2.0e+06	1.9232e+04	4.7315e+03	1.8457e+05	3.9290e+07	1.3926e+07
3.5e+06	1.0990e+04	8.2801e+03	1.0547e+05	6.8757e+07	2.4370e+07
5.0e+06	7.6928e+03	1.1829e+04	7.3828e+04	9.8224e+07	3.4815e+07
6.5e+06	5.9177e+03	1.5377e+04	5.6792e+04	1.2769e+08	4.5258e+07
8.0e+06	4.8076e+03	1.8928e+04	4.6138e+04	1.5717e+08	5.5709e+07
9.5e+06	4.0495e+03	2.2471e+04	3.8863e+04	1.8660e+08	6.6138e+07

Table 3. Case  $M/M_\odot = 0.6$ : Results concerning the perpendicular rotator (part I)

$L_{xx}$	$P_{RR}$	$T_{RR}$	$I_{11}$	$I_{33}$	$\langle H_{ts} \rangle$	$H_{t[\max]}$	$\langle H_t \rangle$	$\omega_e^{-1}$
5.150e+48	218.3990	7.4081e+46	1.7901e+50	1.7210e+50	4.3247e+09	2.6924e+11	1.1691e+11	1.0000
5.500e+48	204.6816	8.4418e+46	1.7917e+50	1.7210e+50	4.3247e+09	2.6924e+11	1.1691e+11	1.0000
6.000e+48	187.8799	1.0033e+47	1.7941e+50	1.7210e+50	4.3247e+09	2.6924e+11	1.1691e+11	1.0000
6.500e+48	173.6831	1.1757e+47	1.7968e+50	1.7210e+50	4.3247e+09	2.6924e+11	1.1691e+11	1.0000
7.000e+48	161.5330	1.3614e+47	1.7996e+50	1.7210e+50	4.3247e+09	2.6924e+11	1.1691e+11	1.0000
7.500e+48	151.0202	1.5602e+47	1.8027e+50	1.7210e+50	4.3247e+09	2.6924e+11	1.1691e+11	1.0000
7.900e+48	143.5799	1.7286e+47	1.8053e+50	1.7210e+50	4.3247e+09	2.6924e+11	1.1691e+11	1.0000

Table 4. Case  $M/M_{\odot} = 0.6$ : Results concerning the perpendicular rotator (part II)

$B_s$	$\beta_*^p$	$V_{As}$	$t_{As}$	$H_p[\max]$	$\langle H_p \rangle$
Models with $L_{xx} = 5.150e+48$					
5.0e+05	7.6963e+04	1.1891e+03	7.3184e+05	9.9651e+06	3.5280e+06
2.0e+06	1.9241e+04	4.7562e+03	1.8297e+05	3.9859e+07	1.4112e+07
3.5e+06	1.0994e+04	8.3242e+03	1.0454e+05	6.9760e+07	2.4698e+07
5.0e+06	7.6962e+03	1.1891e+04	7.3183e+04	9.9653e+07	3.5281e+07
6.5e+06	5.9205e+03	1.5458e+04	5.6297e+04	1.2954e+08	4.5863e+07
8.0e+06	4.8104e+03	1.9025e+04	4.5742e+04	1.5944e+08	5.6447e+07
9.5e+06	4.0513e+03	2.2590e+04	3.8523e+04	1.8931e+08	6.7024e+07
Models with $L_{xx} = 5.500e+48$					
5.0e+05	7.6910e+04	1.1899e+03	7.3134e+05	9.9720e+06	3.5305e+06
2.0e+06	1.9228e+04	4.7595e+03	1.8284e+05	3.9887e+07	1.4122e+07
3.5e+06	1.0986e+04	8.3300e+03	1.0447e+05	6.9809e+07	2.4715e+07
5.0e+06	7.6905e+03	1.1900e+04	7.3129e+04	9.9727e+07	3.5307e+07
6.5e+06	5.9166e+03	1.5468e+04	5.6261e+04	1.2963e+08	4.5893e+07
8.0e+06	4.8066e+03	1.9040e+04	4.5706e+04	1.5956e+08	5.6492e+07
9.6e+06	4.0474e+03	2.2611e+04	3.8487e+04	1.8949e+08	6.7087e+07
Models with $L_{xx} = 6.000e+48$					
5.0e+05	7.6828e+04	1.1912e+03	7.3056e+05	9.9826e+06	3.5343e+06
2.0e+06	1.9207e+04	4.7647e+03	1.8264e+05	3.9931e+07	1.4137e+07
3.5e+06	1.0975e+04	8.3387e+03	1.0436e+05	6.9882e+07	2.4741e+07
5.0e+06	7.6828e+03	1.1912e+04	7.3056e+04	9.9826e+07	3.5342e+07
6.5e+06	5.9090e+03	1.5488e+04	5.6189e+04	1.2979e+08	4.5952e+07
8.1e+06	4.8008e+03	1.9063e+04	4.5651e+04	1.5975e+08	5.6559e+07
9.6e+06	4.0436e+03	2.2632e+04	3.8451e+04	1.8967e+08	6.7150e+07
Models with $L_{xx} = 6.500e+48$					
5.0e+05	7.6738e+04	1.1926e+03	7.2970e+05	9.9943e+06	3.5384e+06
2.0e+06	1.9184e+04	4.7704e+03	1.8242e+05	3.9978e+07	1.4154e+07
3.5e+06	1.0963e+04	8.3474e+03	1.0425e+05	6.9955e+07	2.4767e+07
5.0e+06	7.6733e+03	1.1927e+04	7.2965e+04	9.9950e+07	3.5386e+07
6.6e+06	5.9033e+03	1.5503e+04	5.6134e+04	1.2992e+08	4.5996e+07
8.1e+06	4.7970e+03	1.9078e+04	4.5615e+04	1.5988e+08	5.6604e+07
9.6e+06	4.0379e+03	2.2664e+04	3.8396e+04	1.8994e+08	6.7245e+07
Models with $L_{xx} = 7.000e+48$					
5.0e+05	7.6642e+04	1.1941e+03	7.2879e+05	1.0007e+07	3.5428e+06
2.0e+06	1.9161e+04	4.7761e+03	1.8220e+05	4.0026e+07	1.4171e+07
3.5e+06	1.0948e+04	8.3590e+03	1.0411e+05	7.0052e+07	2.4801e+07
5.0e+06	7.6638e+03	1.1941e+04	7.2875e+04	1.0007e+08	3.5430e+07
6.6e+06	5.8957e+03	1.5523e+04	5.6062e+04	1.3009e+08	4.6056e+07

Table 4—Continued

$B_s$	$\beta_*^p$	$V_{As}$	$t_{As}$	$H_p[\max]$	$\langle H_p \rangle$
8.1e+06	4.7894e+03	1.9108e+04	4.5542e+04	1.6013e+08	5.6694e+07
9.6e+06	4.0341e+03	2.2686e+04	3.8360e+04	1.9012e+08	6.7309e+07
Models with $L_{xx} = 7.500\text{e+48}$					
5.1e+05	7.6540e+04	1.1957e+03	7.2782e+05	1.0020e+07	3.5476e+06
2.0e+06	1.9135e+04	4.7828e+03	1.8195e+05	4.0082e+07	1.4191e+07
3.5e+06	1.0935e+04	8.3692e+03	1.0398e+05	7.0138e+07	2.4832e+07
5.1e+06	7.6542e+03	1.1956e+04	7.2784e+04	1.0020e+08	3.5475e+07
6.6e+06	5.8880e+03	1.5543e+04	5.5989e+04	1.3026e+08	4.6116e+07
8.1e+06	4.7837e+03	1.9131e+04	4.5488e+04	1.6033e+08	5.6762e+07
9.6e+06	4.0284e+03	2.2718e+04	3.8306e+04	1.9039e+08	6.7405e+07
Models with $L_{xx} = 7.900\text{e+48}$					
5.1e+05	7.6452e+04	1.1970e+03	7.2698e+05	1.0032e+07	3.5516e+06
2.0e+06	1.9114e+04	4.7880e+03	1.8175e+05	4.0126e+07	1.4206e+07
3.5e+06	1.0922e+04	8.3794e+03	1.0385e+05	7.0223e+07	2.4862e+07
5.1e+06	7.6447e+03	1.1971e+04	7.2693e+04	1.0032e+08	3.5519e+07
6.6e+06	5.8804e+03	1.5563e+04	5.5917e+04	1.3042e+08	4.6175e+07
8.1e+06	4.7779e+03	1.9154e+04	4.5433e+04	1.6052e+08	5.6830e+07
9.6e+06	4.0245e+03	2.2740e+04	3.8269e+04	1.9057e+08	6.7468e+07

Table 5. Case  $M/M_{\odot} = 0.6$ : Results concerning the turn-over phase

$B_s$	$f$	$t_{\text{TOV}}$	$\dot{P}_{\text{TOV}}$	$N_{xx}$	$t_{\text{now}}$	$\dot{T}$
$L_{xx} = 5.150\text{e}+48, A_r = 1.0065, \chi_{\text{now}} = 6.5298, F_{r[\text{now}]} = 0.9938$						
5.0e+05	3.9951e+23	7.3392e+09	3.3207e-16	1.6352e+15	4.3666e+07	2.6338e+28
2.0e+06	1.5980e+24	4.4475e+08	5.4797e-15	9.9090e+13	2.6461e+06	4.3463e+29
3.5e+06	2.7966e+24	1.4995e+08	1.6252e-14	3.3410e+13	8.9218e+05	1.2891e+30
5.0e+06	3.9951e+24	7.0972e+07	3.4339e-14	1.5813e+13	4.2227e+05	2.7236e+30
6.5e+06	5.1936e+24	4.1868e+07	5.8208e-14	9.3284e+12	2.4911e+05	4.6169e+30
8.0e+06	6.3921e+24	2.7635e+07	8.8189e-14	6.1571e+12	1.6442e+05	6.9948e+30
9.5e+06	7.5907e+24	1.9571e+07	1.2452e-13	4.3606e+12	1.1645e+05	9.8767e+30
$L_{xx} = 5.500\text{e}+48, A_r = 1.0074, \chi_{\text{now}} = 32.2461, F_{r[\text{now}]} = 0.8460$						
5.0e+05	3.9979e+23	5.5981e+09	4.1102e-16	1.3362e+15	7.6225e+08	3.9311e+28
2.0e+06	1.5992e+24	3.3927e+08	6.7819e-15	8.0982e+13	4.6196e+07	6.4864e+29
3.5e+06	2.7985e+24	1.1438e+08	2.0117e-14	2.7301e+13	1.5574e+07	1.9240e+30
5.0e+06	3.9979e+24	5.4146e+07	4.2495e-14	1.2924e+13	7.3726e+06	4.0643e+30
6.5e+06	5.1972e+24	3.1937e+07	7.2045e-14	7.6232e+12	4.3487e+06	6.8906e+30
8.0e+06	6.3966e+24	2.1077e+07	1.0917e-13	5.0310e+12	2.8699e+06	1.0441e+31
9.5e+06	7.5960e+24	1.4939e+07	1.5403e-13	3.5657e+12	2.0341e+06	1.4731e+31
$L_{xx} = 6.000\text{e}+48, A_r = 1.0087, \chi_{\text{now}} = 51.9417, F_{r[\text{now}]} = 0.6166$						
5.0e+05	4.0022e+23	3.9250e+09	5.4216e-16	1.0249e+15	1.2416e+09	6.6504e+28
2.0e+06	1.6009e+24	2.3789e+08	8.9453e-15	6.2117e+13	7.5250e+07	1.0973e+30
3.5e+06	2.8015e+24	8.0195e+07	2.6535e-14	2.0941e+13	2.5368e+07	3.2549e+30
5.0e+06	4.0022e+24	3.7948e+07	5.6076e-14	9.9089e+12	1.2004e+07	6.8786e+30
6.5e+06	5.2028e+24	2.2387e+07	9.5054e-14	5.8457e+12	7.0816e+06	1.1660e+31
8.0e+06	6.4035e+24	1.4782e+07	1.4396e-13	3.8598e+12	4.6758e+06	1.7659e+31
9.5e+06	7.6041e+24	1.0475e+07	2.0315e-13	2.7352e+12	3.3135e+06	2.4919e+31
$L_{xx} = 6.500\text{e}+48, A_r = 1.0102, \chi_{\text{now}} = 66.4632, F_{r[\text{now}]} = 0.3995$						
5.0e+05	4.0068e+23	2.8474e+09	6.9234e-16	8.0525e+14	1.3963e+09	1.0715e+29
2.0e+06	1.6027e+24	1.7257e+08	1.1424e-14	4.8803e+13	8.4625e+07	1.7679e+30
3.5e+06	2.8048e+24	5.8165e+07	3.3893e-14	1.6449e+13	2.8522e+07	5.2453e+30
5.0e+06	4.0068e+24	2.7534e+07	7.1598e-14	7.7866e+12	1.3502e+07	1.1080e+31
6.5e+06	5.2089e+24	1.6239e+07	1.2140e-13	4.5923e+12	7.9630e+06	1.8788e+31
8.0e+06	6.4109e+24	1.0727e+07	1.8377e-13	3.0337e+12	5.2604e+06	2.8441e+31
9.5e+06	7.6130e+24	7.5938e+06	2.5960e-13	2.1475e+12	3.7238e+06	4.0176e+31
$L_{xx} = 7.000\text{e}+48, A_r = 1.0118, \chi_{\text{now}} = 77.2625, F_{r[\text{now}]} = 0.2206$						
5.0e+05	4.0118e+23	2.1235e+09	8.6058e-16	6.4451e+14	1.4038e+09	1.6584e+29
2.0e+06	1.6047e+24	1.2871e+08	1.4199e-14	3.9064e+13	8.5082e+07	2.7361e+30
3.5e+06	2.8083e+24	4.3386e+07	4.2121e-14	1.3168e+13	2.8681e+07	8.1168e+30
5.0e+06	4.0118e+24	2.0539e+07	8.8974e-14	6.2338e+12	1.3577e+07	1.7146e+31
6.5e+06	5.2154e+24	1.2110e+07	1.5091e-13	3.6754e+12	8.0052e+06	2.9081e+31

Table 5—Continued

$B_s$	$f$	$t_{\text{TOV}}$	$\dot{P}_{\text{TOV}}$	$N_{xx}$	$t_{\text{now}}$	$\dot{T}$
8.0e+06	6.4190e+24	7.9974e+06	2.2850e-13	2.4273e+12	5.2868e+06	4.4033e+31
9.5e+06	7.6225e+24	5.6648e+06	3.2259e-13	1.7194e+12	3.7448e+06	6.2165e+31
$L_{xx} = 7.500\text{e}+48, A_r = 1.0136, \chi_{\text{now}} = 84.9531, F_{r[\text{now}]} = 0.0880$						
5.0e+05	4.0172e+23	1.6251e+09	1.0471e-15	5.2640e+14	1.3519e+09	2.4750e+29
2.0e+06	1.6069e+24	9.8489e+07	1.7278e-14	3.1903e+13	8.1934e+07	4.0838e+30
3.5e+06	2.8121e+24	3.3200e+07	5.1256e-14	1.0754e+13	2.7619e+07	1.2115e+31
5.0e+06	4.0172e+24	1.5716e+07	1.0828e-13	5.0906e+12	1.3074e+07	2.5593e+31
6.5e+06	5.2224e+24	9.2674e+06	1.8362e-13	3.0019e+12	7.7096e+06	4.3401e+31
8.0e+06	6.4276e+24	6.1187e+06	2.7811e-13	1.9820e+12	5.0902e+06	6.5734e+31
9.5e+06	7.6327e+24	4.3368e+06	3.9238e-13	1.4048e+12	3.6078e+06	9.2744e+31
$L_{xx} = 7.900\text{e}+48, A_r = 1.0150, \chi_{\text{now}} = 89.2287, F_{r[\text{now}]} = 0.0135$						
5.0e+05	4.0218e+23	1.3288e+09	1.2182e-15	4.5290e+14	1.2877e+09	3.3443e+29
2.0e+06	1.6087e+24	8.0547e+07	2.0097e-14	2.7452e+13	7.8054e+07	5.5173e+30
3.5e+06	2.8152e+24	2.7150e+07	5.9624e-14	9.2532e+12	2.6310e+07	1.6368e+31
5.0e+06	4.0218e+24	1.2853e+07	1.2595e-13	4.3804e+12	1.2455e+07	3.4577e+31
6.5e+06	5.2283e+24	7.5816e+06	2.1351e-13	2.5840e+12	7.3470e+06	5.8616e+31
8.0e+06	6.4348e+24	5.0050e+06	3.2343e-13	1.7058e+12	4.8501e+06	8.8791e+31
9.5e+06	7.6414e+24	3.5469e+06	4.5639e-13	1.2088e+12	3.4371e+06	1.2529e+32

Note. —  $t_{\text{TOV}}$  and  $t_{\text{now}}$  are given in years.  $\chi_{\text{now}}$  is given in arcdegrees.

Table 6. Case  $M/M_\odot = 0.9$ : Results concerning the aligned rotator (part I)

$L_{xx}$	$P_{xx}$	$T_{xx}$	$I_{11}$	$I_{33}$	$\langle H_{ts} \rangle$	$H_{t[\text{max}]}$	$\langle H_t \rangle$	$\omega_e^{-1}$
1.620e+49	32.9038	1.0425e+48	1.3595e+50	1.3358e+50	2.7897e+09	7.9651e+11	3.2773e+11	3.6838
1.650e+49	31.9878	1.0799e+48	1.3608e+50	1.3378e+50	2.7908e+09	7.9549e+11	3.2733e+11	3.6830
1.850e+49	28.6012	1.3434e+48	1.3705e+50	1.3519e+50	2.7979e+09	7.8823e+11	3.2454e+11	3.6777
2.050e+49	26.0253	1.6305e+48	1.3812e+50	1.3676e+50	2.8057e+09	7.8033e+11	3.2149e+11	3.6724
2.250e+49	24.0878	1.9393e+48	1.3930e+50	1.3848e+50	2.8142e+09	7.7184e+11	3.1821e+11	3.6664
2.450e+49	22.6166	2.2683e+48	1.4057e+50	1.4035e+50	2.8234e+09	7.6283e+11	3.1473e+11	3.6599
2.515e+49	22.1804	2.3792e+48	1.4100e+50	1.4099e+50	2.8265e+09	7.5981e+11	3.1356e+11	3.6575

Table 7. Case  $M/M_{\odot} = 0.9$ : Results concerning the aligned rotator (part II)

$B_s$	$\beta_*^p$	$V_{As}$	$t_{As}$	$H_p[\max]$	$\langle H_p \rangle$
Models with $L_{xx} = 1.620e+49$					
5.0e+05	1.0210e+05	1.2872e+03	5.0307e+05	2.3724e+07	7.5225e+06
2.0e+06	2.5526e+04	5.1488e+03	1.2577e+05	9.4895e+07	3.0089e+07
3.5e+06	1.4586e+04	9.0102e+03	7.1870e+04	1.6606e+08	5.2655e+07
5.0e+06	1.0209e+04	1.2873e+04	5.0303e+04	2.3726e+08	7.5231e+07
6.5e+06	7.8548e+03	1.6732e+04	3.8702e+04	3.0838e+08	9.7781e+07
8.0e+06	6.3815e+03	2.0595e+04	3.1443e+04	3.7958e+08	1.2036e+08
9.5e+06	5.3738e+03	2.4457e+04	2.6478e+04	4.5075e+08	1.4293e+08
Models with $L_{xx} = 1.650e+49$					
5.0e+05	1.0207e+05	1.2872e+03	5.0326e+05	2.3699e+07	7.5155e+06
2.0e+06	2.5518e+04	5.1489e+03	1.2581e+05	9.4796e+07	3.0062e+07
3.5e+06	1.4583e+04	9.0101e+03	7.1897e+04	1.6588e+08	5.2606e+07
5.0e+06	1.0207e+04	1.2872e+04	5.0325e+04	2.3699e+08	7.5156e+07
6.5e+06	7.8511e+03	1.6735e+04	3.8708e+04	3.0811e+08	9.7711e+07
8.0e+06	6.3796e+03	2.0596e+04	3.1454e+04	3.7918e+08	1.2025e+08
9.5e+06	5.3719e+03	2.4459e+04	2.6485e+04	4.5031e+08	1.4281e+08
Models with $L_{xx} = 1.850e+49$					
5.0e+05	1.0188e+05	1.2872e+03	5.0460e+05	2.3519e+07	7.4665e+06
2.0e+06	2.5470e+04	5.1489e+03	1.2615e+05	9.4074e+07	2.9866e+07
3.5e+06	1.4555e+04	9.0102e+03	7.2088e+04	1.6462e+08	5.2264e+07
5.0e+06	1.0189e+04	1.2871e+04	5.0464e+04	2.3517e+08	7.4659e+07
6.5e+06	7.8362e+03	1.6735e+04	3.8812e+04	3.0577e+08	9.7073e+07
8.0e+06	6.3666e+03	2.0598e+04	3.1533e+04	3.7635e+08	1.1948e+08
9.5e+06	5.3626e+03	2.4455e+04	2.6561e+04	4.4681e+08	1.4185e+08
Models with $L_{xx} = 2.050e+49$					
5.0e+05	1.0167e+05	1.2872e+03	5.0608e+05	2.3322e+07	7.4130e+06
2.0e+06	2.5416e+04	5.1490e+03	1.2652e+05	9.3290e+07	2.9653e+07
3.5e+06	1.4523e+04	9.0108e+03	7.2294e+04	1.6326e+08	5.1893e+07
5.0e+06	1.0166e+04	1.2872e+04	5.0607e+04	2.3322e+08	7.4131e+07
6.5e+06	7.8213e+03	1.6732e+04	3.8934e+04	3.0315e+08	9.6358e+07
8.0e+06	6.3536e+03	2.0597e+04	3.1627e+04	3.7318e+08	1.1862e+08
9.5e+06	5.3514e+03	2.4454e+04	2.6639e+04	4.4306e+08	1.4083e+08
Models with $L_{xx} = 2.250e+49$					
5.0e+05	1.0143e+05	1.2872e+03	5.0769e+05	2.3111e+07	7.3556e+06
2.0e+06	2.5358e+04	5.1487e+03	1.2692e+05	9.2443e+07	2.9422e+07
3.5e+06	1.4490e+04	9.0108e+03	7.2524e+04	1.6178e+08	5.1491e+07
5.0e+06	1.0142e+04	1.2873e+04	5.0764e+04	2.3113e+08	7.3562e+07
6.5e+06	7.8027e+03	1.6733e+04	3.9055e+04	3.0043e+08	9.5618e+07

Table 7—Continued

$B_s$	$\beta_*^p$	$V_{As}$	$t_{As}$	$H_p[\max]$	$\langle H_p \rangle$
8.0e+06	6.3387e+03	2.0598e+04	3.1727e+04	3.6982e+08	1.1770e+08
9.5e+06	5.3384e+03	2.4457e+04	2.6720e+04	4.3912e+08	1.3976e+08
Models with $L_{xx} = 2.450\text{e+49}$					
5.0e+05	1.0118e+05	1.2872e+03	5.0941e+05	2.2888e+07	7.2945e+06
2.0e+06	2.5295e+04	5.1487e+03	1.2736e+05	9.1548e+07	2.9177e+07
3.5e+06	1.4454e+04	9.0103e+03	7.2775e+04	1.6021e+08	5.1060e+07
5.0e+06	1.0118e+04	1.2872e+04	5.0943e+04	2.2887e+08	7.2943e+07
6.5e+06	7.7822e+03	1.6735e+04	3.9182e+04	2.9756e+08	9.4836e+07
8.0e+06	6.3237e+03	2.0595e+04	3.1839e+04	3.6619e+08	1.1671e+08
9.5e+06	5.3254e+03	2.4456e+04	2.6813e+04	4.3484e+08	1.3859e+08
Models with $L_{xx} = 2.515\text{e+49}$					
5.0e+05	1.0109e+05	1.2872e+03	5.0999e+05	2.2813e+07	7.2740e+06
2.0e+06	2.5272e+04	5.1489e+03	1.2750e+05	9.1251e+07	2.9096e+07
3.5e+06	1.4441e+04	9.0107e+03	7.2855e+04	1.5969e+08	5.0919e+07
5.0e+06	1.0109e+04	1.2873e+04	5.0998e+04	2.2813e+08	7.2742e+07
6.5e+06	7.7766e+03	1.6733e+04	3.9233e+04	2.9655e+08	9.4556e+07
8.0e+06	6.3182e+03	2.0595e+04	3.1875e+04	3.6500e+08	1.1638e+08
9.5e+06	5.3198e+03	2.4461e+04	2.6838e+04	4.3350e+08	1.3823e+08

Table 8. Case  $M/M_\odot = 0.9$ : Results concerning the perpendicular rotator (part I)

$L_{xx}$	$P_{RR}$	$T_{RR}$	$I_{11}$	$I_{33}$	$\langle H_{ts} \rangle$	$H_{t[\max]}$	$\langle H_t \rangle$	$\omega_e^{-1}$
1.620e+49	53.1206	9.5808e+47	1.3696e+50	1.2828e+50	2.7624e+09	8.2518e+11	3.3875e+11	1.0000
1.650e+49	52.2320	9.9242e+47	1.3716e+50	1.2828e+50	2.7624e+09	8.2518e+11	3.3875e+11	1.0000
1.850e+49	46.9921	1.2368e+48	1.3836e+50	1.2828e+50	2.7624e+09	8.2518e+11	3.3875e+11	1.0000
2.050e+49	42.8154	1.5042e+48	1.3969e+50	1.2828e+50	2.7624e+09	8.2518e+11	3.3875e+11	1.0000
2.250e+49	39.4104	1.7936e+48	1.4113e+50	1.2828e+50	2.7624e+09	8.2518e+11	3.3875e+11	1.0000
2.450e+49	36.5795	2.1042e+48	1.4263e+50	1.2828e+50	2.7624e+09	8.2518e+11	3.3875e+11	1.0000
2.515e+49	35.7638	2.2092e+48	1.4315e+50	1.2828e+50	2.7624e+09	8.2518e+11	3.3875e+11	1.0000

Table 9. Case  $M/M_{\odot} = 0.9$ : Results concerning the perpendicular rotator (part II)

$B_s$	$\beta_*^p$	$V_{As}$	$t_{As}$	$H_p[\max]$	$\langle H_p \rangle$
Models with $L_{xx} = 1.620e+49$					
5.1e+05	9.9861e+04	1.3256e+03	4.8349e+05	2.5165e+07	7.9456e+06
2.1e+06	2.4965e+04	5.3025e+03	1.2087e+05	1.0066e+08	3.1783e+07
3.6e+06	1.4265e+04	9.2799e+03	6.9067e+04	1.7617e+08	5.5623e+07
5.1e+06	9.9869e+03	1.3255e+04	4.8353e+04	2.5163e+08	7.9450e+07
6.7e+06	7.6809e+03	1.7235e+04	3.7188e+04	3.2718e+08	1.0330e+08
8.2e+06	6.2409e+03	2.1211e+04	3.0216e+04	4.0267e+08	1.2714e+08
9.8e+06	5.2567e+03	2.5183e+04	2.5451e+04	4.7806e+08	1.5094e+08
Models with $L_{xx} = 1.650e+49$					
5.2e+05	9.9754e+04	1.3270e+03	4.8297e+05	2.5192e+07	7.9542e+06
2.1e+06	2.4939e+04	5.3082e+03	1.2074e+05	1.0077e+08	3.1817e+07
3.6e+06	1.4250e+04	9.2898e+03	6.8993e+04	1.7635e+08	5.5682e+07
5.2e+06	9.9755e+03	1.3270e+04	4.8298e+04	2.5192e+08	7.9541e+07
6.7e+06	7.6733e+03	1.7252e+04	3.7151e+04	3.2750e+08	1.0341e+08
8.2e+06	6.2352e+03	2.1231e+04	3.0188e+04	4.0304e+08	1.2726e+08
9.8e+06	5.2510e+03	2.5210e+04	2.5423e+04	4.7858e+08	1.5111e+08
Models with $L_{xx} = 1.850e+49$					
5.2e+05	9.8996e+04	1.3372e+03	4.7930e+05	2.5385e+07	8.0151e+06
2.1e+06	2.4750e+04	5.3487e+03	1.1983e+05	1.0154e+08	3.2059e+07
3.6e+06	1.4143e+04	9.3600e+03	6.8476e+04	1.7769e+08	5.6103e+07
5.2e+06	9.8992e+03	1.3373e+04	4.7928e+04	2.5386e+08	8.0154e+07
6.8e+06	7.6142e+03	1.7386e+04	3.6865e+04	3.3004e+08	1.0421e+08
8.3e+06	6.1875e+03	2.1395e+04	2.9958e+04	4.0615e+08	1.2824e+08
9.9e+06	5.2109e+03	2.5404e+04	2.5229e+04	4.8226e+08	1.5227e+08
Models with $L_{xx} = 2.050e+49$					
5.2e+05	9.8169e+04	1.3485e+03	4.7530e+05	2.5599e+07	8.0826e+06
2.1e+06	2.4542e+04	5.3940e+03	1.1882e+05	1.0240e+08	3.2331e+07
3.7e+06	1.4025e+04	9.4389e+03	6.7903e+04	1.7918e+08	5.6576e+07
5.2e+06	9.8172e+03	1.3484e+04	4.7531e+04	2.5598e+08	8.0824e+07
6.8e+06	7.5512e+03	1.7531e+04	3.6560e+04	3.3280e+08	1.0508e+08
8.4e+06	6.1360e+03	2.1574e+04	2.9708e+04	4.0955e+08	1.2931e+08
1.0e+07	5.1670e+03	2.5620e+04	2.5017e+04	4.8635e+08	1.5356e+08
Models with $L_{xx} = 2.250e+49$					
5.3e+05	9.7280e+04	1.3608e+03	4.7100e+05	2.5833e+07	8.1564e+06
2.1e+06	2.4321e+04	5.4430e+03	1.1775e+05	1.0333e+08	3.2625e+07
3.7e+06	1.3897e+04	9.5257e+03	6.7284e+04	1.8083e+08	5.7096e+07
5.3e+06	9.7275e+03	1.3609e+04	4.7097e+04	2.5834e+08	8.1569e+07
6.9e+06	7.4826e+03	1.7692e+04	3.6228e+04	3.3585e+08	1.0604e+08

Table 9—Continued

$B_s$	$\beta_*^p$	$V_{As}$	$t_{As}$	$H_p[\max]$	$\langle H_p \rangle$
8.5e+06	6.0807e+03	2.1770e+04	2.9440e+04	4.1328e+08	1.3049e+08
1.0e+07	5.1194e+03	2.5858e+04	2.4786e+04	4.9088e+08	1.5499e+08
Models with $L_{xx} = 2.450\text{e+49}$					
5.3e+05	9.6336e+04	1.3741e+03	4.6643e+05	2.6086e+07	8.2364e+06
2.1e+06	2.4084e+04	5.4965e+03	1.1661e+05	1.0434e+08	3.2945e+07
3.7e+06	1.3762e+04	9.6194e+03	6.6629e+04	1.8261e+08	5.7658e+07
5.3e+06	9.6341e+03	1.3741e+04	4.6645e+04	2.6085e+08	8.2360e+07
6.9e+06	7.4101e+03	1.7865e+04	3.5877e+04	3.3913e+08	1.0708e+08
8.5e+06	6.0215e+03	2.1984e+04	2.9154e+04	4.1734e+08	1.3177e+08
1.0e+07	5.0698e+03	2.6111e+04	2.4546e+04	4.9569e+08	1.5651e+08
Models with $L_{xx} = 2.515\text{e+49}$					
5.4e+05	9.6019e+04	1.3787e+03	4.6489e+05	2.6172e+07	8.2636e+06
2.1e+06	2.4004e+04	5.5148e+03	1.1622e+05	1.0469e+08	3.3055e+07
3.7e+06	1.3718e+04	9.6502e+03	6.6416e+04	1.8320e+08	5.7842e+07
5.4e+06	9.6016e+03	1.3787e+04	4.6488e+04	2.6173e+08	8.2638e+07
7.0e+06	7.3853e+03	1.7925e+04	3.5757e+04	3.4027e+08	1.0744e+08
8.6e+06	6.0006e+03	2.2061e+04	2.9053e+04	4.1880e+08	1.3223e+08
1.0e+07	5.0545e+03	2.6190e+04	2.4472e+04	4.9718e+08	1.5698e+08

Table 10. Case  $M/M_{\odot} = 0.9$ : Results concerning the turn-over phase

$B_s$	$f$	$t_{\text{TOV}}$	$\dot{P}_{\text{TOV}}$	$N_{xx}$	$t_{\text{now}}$	$\dot{T}$
$L_{xx} = 1.620\text{e+49}, A_r = 1.0352, \chi_{\text{now}} = 5.7116, F_{r[\text{now}]} = 0.9953$						
5.0e+05	2.2252e+23	8.5891e+08	7.4638e-16	8.2321e+14	4.0878e+06	3.1183e+30
2.0e+06	8.9010e+23	5.5703e+07	1.1509e-14	5.3388e+13	2.6510e+05	4.8082e+31
3.5e+06	1.5577e+24	1.8184e+07	3.5254e-14	1.7428e+13	8.6542e+04	1.4729e+32
5.0e+06	2.2252e+24	8.9203e+06	7.1866e-14	8.5495e+12	4.2454e+04	3.0025e+32
6.5e+06	2.8928e+24	5.0956e+06	1.2581e-13	4.8838e+12	2.4251e+04	5.2562e+32
8.0e+06	3.5604e+24	3.4816e+06	1.8413e-13	3.3369e+12	1.6570e+04	7.6928e+32
9.5e+06	4.2280e+24	2.3813e+06	2.6921e-13	2.2823e+12	1.1333e+04	1.1247e+33
$L_{xx} = 1.650\text{e+49}, A_r = 1.0368, \chi_{\text{now}} = 18.6915, F_{r[\text{now}]} = 0.9475$						
5.0e+05	2.2276e+23	7.8942e+08	8.1317e-16	7.7827e+14	3.9469e+07	3.5158e+30
2.0e+06	8.9105e+23	5.1193e+07	1.2540e-14	5.0470e+13	2.5595e+06	5.4215e+31
3.5e+06	1.5593e+24	1.6713e+07	3.8410e-14	1.6477e+13	8.3561e+05	1.6606e+32
5.0e+06	2.2276e+24	8.1998e+06	7.8287e-14	8.0840e+12	4.0997e+05	3.3847e+32
6.5e+06	2.8959e+24	4.6813e+06	1.3713e-13	4.6152e+12	2.3405e+05	5.9287e+32
8.0e+06	3.5642e+24	3.1997e+06	2.0062e-13	3.1545e+12	1.5998e+05	8.6739e+32
9.5e+06	4.2325e+24	2.1882e+06	2.9336e-13	2.1573e+12	1.0941e+05	1.2683e+33
$L_{xx} = 1.850\text{e+49}, A_r = 1.0458, \chi_{\text{now}} = 46.6186, F_{r[\text{now}]} = 0.6871$						
5.0e+05	2.2447e+23	5.1969e+08	1.1222e-15	5.7301e+14	1.2430e+08	6.5064e+30
2.0e+06	8.9787e+23	3.3702e+07	1.7304e-14	3.7160e+13	8.0610e+06	1.0033e+32
3.5e+06	1.5713e+24	1.1002e+07	5.3004e-14	1.2131e+13	2.6316e+06	3.0732e+32
5.0e+06	2.2447e+24	5.3990e+06	1.0801e-13	5.9530e+12	1.2914e+06	6.2628e+32
6.5e+06	2.9181e+24	3.0819e+06	1.8922e-13	3.3982e+12	7.3715e+05	1.0971e+33
8.0e+06	3.5915e+24	2.1059e+06	2.7692e-13	2.3220e+12	5.0370e+05	1.6056e+33
9.5e+06	4.2649e+24	1.4411e+06	4.0467e-13	1.5890e+12	3.4468e+05	2.3463e+33
$L_{xx} = 2.050\text{e+49}, A_r = 1.0559, \chi_{\text{now}} = 65.6329, F_{r[\text{now}]} = 0.4127$						
5.0e+05	2.2636e+23	3.5785e+08	1.4878e-15	4.3363e+14	1.4865e+08	1.1190e+31
2.0e+06	9.0543e+23	2.3206e+07	2.2943e-14	2.8120e+13	9.6400e+06	1.7255e+32
3.5e+06	1.5845e+24	7.5752e+06	7.0284e-14	9.1792e+12	3.1468e+06	5.2861e+32
5.0e+06	2.2636e+24	3.7170e+06	1.4324e-13	4.5041e+12	1.5441e+06	1.0773e+33
6.5e+06	2.9426e+24	2.1231e+06	2.5077e-13	2.5727e+12	8.8195e+05	1.8861e+33
8.0e+06	3.6217e+24	1.4503e+06	3.6711e-13	1.7574e+12	6.0245e+05	2.7611e+33
9.5e+06	4.3008e+24	9.9237e+05	5.3651e-13	1.2025e+12	4.1224e+05	4.0351e+33
$L_{xx} = 2.250\text{e+49}, A_r = 1.0667, \chi_{\text{now}} = 78.0010, F_{r[\text{now}]} = 0.2080$						
5.0e+05	2.2842e+23	2.4721e+08	1.9654e-15	3.2365e+14	1.4379e+08	1.8697e+31
2.0e+06	9.1370e+23	1.6032e+07	3.0306e-14	2.0990e+13	9.3251e+06	2.8830e+32
3.5e+06	1.5990e+24	5.2331e+06	9.2847e-14	6.8512e+12	3.0438e+06	8.8325e+32
5.0e+06	2.2842e+24	2.5674e+06	1.8925e-13	3.3612e+12	1.4933e+06	1.8003e+33
6.5e+06	2.9695e+24	1.4665e+06	3.3132e-13	1.9200e+12	8.5297e+05	3.1518e+33

Table 10—Continued

$B_s$	$f$	$t_{\text{TOV}}$	$\dot{P}_{\text{TOV}}$	$N_{xx}$	$t_{\text{now}}$	$\dot{T}$
8.0e+06	3.6548e+24	1.0018e+06	4.8500e-13	1.3116e+12	5.8269e+05	4.6138e+33
9.5e+06	4.3401e+24	6.8537e+05	7.0892e-13	8.9730e+11	3.9864e+05	6.7439e+33
$L_{xx} = 2.450\text{e}+49, A_r = 1.0781, \chi_{\text{now}} = 85.1031, F_{r[\text{now}]} = 0.0854$						
5.0e+05	2.3066e+23	1.6364e+08	2.7057e-15	2.2817e+14	1.2169e+08	3.1806e+31
2.0e+06	9.2266e+23	1.0612e+07	4.1721e-14	1.4798e+13	7.8918e+06	4.9043e+32
3.5e+06	1.6146e+24	3.4643e+06	1.2780e-13	4.8306e+12	2.5762e+06	1.5024e+33
5.0e+06	2.3066e+24	1.6998e+06	2.6048e-13	2.3702e+12	1.2640e+06	3.0619e+33
6.5e+06	2.9986e+24	9.7051e+05	4.5621e-13	1.3533e+12	7.2171e+05	5.3628e+33
8.0e+06	3.6906e+24	6.6332e+05	6.6749e-13	9.2492e+11	4.9328e+05	7.8463e+33
9.5e+06	4.3826e+24	4.5373e+05	9.7583e-13	6.3266e+11	3.3741e+05	1.1471e+34
$L_{xx} = 2.515\text{e}+49, A_r = 1.0821, \chi_{\text{now}} = 86.6041, F_{r[\text{now}]} = 0.0593$						
5.0e+05	2.3143e+23	1.4302e+08	3.0116e-15	2.0335e+14	1.1392e+08	3.7690e+31
2.0e+06	9.2571e+23	9.2751e+06	4.6439e-14	1.3187e+13	7.3879e+06	5.8119e+32
3.5e+06	1.6200e+24	3.0277e+06	1.4226e-13	4.3048e+12	2.4117e+06	1.7804e+33
5.0e+06	2.3143e+24	1.4855e+06	2.8996e-13	2.1121e+12	1.1832e+06	3.6288e+33
6.5e+06	3.0086e+24	8.4850e+05	5.0763e-13	1.2064e+12	6.7586e+05	6.3530e+33
8.0e+06	3.7028e+24	5.7974e+05	7.4297e-13	8.2427e+11	4.6178e+05	9.2982e+33
9.5e+06	4.3971e+24	3.9642e+05	1.0865e-12	5.6363e+11	3.1576e+05	1.3598e+34

Table 11. Case  $M/M_\odot = 1.32$ : Results concerning the aligned rotator (part I)

$L_{xx}$	$P_{xx}$	$T_{xx}$	$I_{11}$	$I_{33}$	$\langle H_{ts} \rangle$	$H_{t[\text{max}]}$	$\langle H_t \rangle$	$\omega_e^{-1}$
1.450e+49	7.9869	3.4198e+48	3.4681e+49	3.4068e+49	1.1345e+09	7.6962e+12	2.6052e+12	5.5989
1.500e+49	7.7621	3.6403e+48	3.4844e+49	3.4246e+49	1.1366e+09	7.6564e+12	2.5930e+12	5.5919
1.800e+49	6.7139	5.0661e+48	3.5905e+49	3.5413e+49	1.1505e+09	7.4057e+12	2.5160e+12	5.5593
2.100e+49	5.9828	6.6382e+48	3.7117e+49	3.6756e+49	1.1660e+09	7.1377e+12	2.4335e+12	5.5200
2.400e+49	5.4567	8.3170e+48	3.8489e+49	3.8283e+49	1.1831e+09	6.8549e+12	2.3461e+12	5.4845
2.700e+49	5.0875	1.0073e+49	4.0003e+49	3.9979e+49	1.2016e+09	6.5663e+12	2.2566e+12	5.4371
2.730e+49	5.0569	1.0252e+49	4.0161e+49	4.0158e+49	1.2035e+09	6.5374e+12	2.2476e+12	5.4312

Table 12. Case  $M/M_{\odot} = 1.32$ : Results concerning the aligned rotator (part II)

$B_s$	$\beta_*^p$	$V_{As}$	$t_{As}$	$H_p[\max]$	$\langle H_p \rangle$
Models with $L_{xx} = 1.450e+49$					
5.0e+05	1.1063e+05	1.4001e+03	2.1902e+05	2.2045e+08	5.2208e+07
2.0e+06	2.7657e+04	5.6004e+03	5.4756e+04	8.8179e+08	2.0883e+08
3.5e+06	1.5803e+04	9.8013e+03	3.1287e+04	1.5432e+09	3.6548e+08
5.0e+06	1.1062e+04	1.4001e+04	2.1902e+04	2.2045e+09	5.2209e+08
6.5e+06	8.5105e+03	1.8200e+04	1.6849e+04	2.8656e+09	6.7864e+08
8.0e+06	6.9142e+03	2.2401e+04	1.3689e+04	3.5271e+09	8.3532e+08
9.5e+06	5.8227e+03	2.6601e+04	1.1528e+04	4.1883e+09	9.9191e+08
Models with $L_{xx} = 1.500e+49$					
5.0e+05	1.1064e+05	1.4001e+03	2.1944e+05	2.1926e+08	5.1959e+07
2.0e+06	2.7660e+04	5.6006e+03	5.4858e+04	8.7709e+08	2.0784e+08
3.5e+06	1.5806e+04	9.8007e+03	3.1349e+04	1.5348e+09	3.6371e+08
5.0e+06	1.1064e+04	1.4001e+04	2.1943e+04	2.1927e+09	5.1960e+08
6.5e+06	8.5105e+03	1.8203e+04	1.6879e+04	2.8507e+09	6.7552e+08
8.0e+06	6.9161e+03	2.2399e+04	1.3716e+04	3.5079e+09	8.3125e+08
9.5e+06	5.8227e+03	2.6605e+04	1.1548e+04	4.1665e+09	9.8734e+08
Models with $L_{xx} = 1.800e+49$					
5.0e+05	1.1076e+05	1.4001e+03	2.2214e+05	2.1182e+08	5.0387e+07
2.0e+06	2.7690e+04	5.6006e+03	5.5532e+04	8.4729e+08	2.0155e+08
3.5e+06	1.5823e+04	9.8009e+03	3.1733e+04	1.4827e+09	3.5271e+08
5.0e+06	1.1077e+04	1.4000e+04	2.2215e+04	2.1180e+09	5.0383e+08
6.5e+06	8.5198e+03	1.8202e+04	1.7086e+04	2.7538e+09	6.5506e+08
8.0e+06	6.9235e+03	2.2399e+04	1.3885e+04	3.3887e+09	8.0610e+08
9.5e+06	5.8301e+03	2.6600e+04	1.1692e+04	4.0242e+09	9.5727e+08
Models with $L_{xx} = 2.100e+49$					
5.0e+05	1.1089e+05	1.4001e+03	2.2515e+05	2.0388e+08	4.8705e+07
2.0e+06	2.7722e+04	5.6006e+03	5.6286e+04	8.1553e+08	1.9483e+08
3.5e+06	1.5842e+04	9.8005e+03	3.2165e+04	1.4271e+09	3.4093e+08
5.0e+06	1.1088e+04	1.4002e+04	2.2514e+04	2.0389e+09	4.8708e+08
6.5e+06	8.5291e+03	1.8203e+04	1.7317e+04	2.6507e+09	6.3323e+08
8.0e+06	6.9310e+03	2.2401e+04	1.4072e+04	3.2619e+09	7.7925e+08
9.5e+06	5.8357e+03	2.6605e+04	1.1849e+04	3.8741e+09	9.2549e+08
Models with $L_{xx} = 2.400e+49$					
5.0e+05	1.1102e+05	1.4001e+03	2.2849e+05	1.9553e+08	4.6931e+07
2.0e+06	2.7755e+04	5.6003e+03	5.7124e+04	7.8209e+08	1.8772e+08
3.5e+06	1.5860e+04	9.8004e+03	3.2643e+04	1.3686e+09	3.2850e+08
5.0e+06	1.1101e+04	1.4002e+04	2.2848e+04	1.9553e+09	4.6933e+08
6.5e+06	8.5403e+03	1.8201e+04	1.7577e+04	2.5417e+09	6.1007e+08

Table 12—Continued

$B_s$	$\beta_*^p$	$V_{As}$	$t_{As}$	$H_p[\max]$	$\langle H_p \rangle$
8.0e+06	6.9384e+03	2.2403e+04	1.4280e+04	3.1285e+09	7.5092e+08
9.5e+06	5.8432e+03	2.6602e+04	1.2026e+04	3.7149e+09	8.9167e+08
Models with $L_{xx} = 2.700\text{e+49}$					
5.0e+05	1.1115e+05	1.4001e+03	2.3209e+05	1.8703e+08	4.5117e+07
2.0e+06	2.7787e+04	5.6005e+03	5.8022e+04	7.4811e+08	1.8047e+08
3.5e+06	1.5879e+04	9.8003e+03	3.3157e+04	1.3091e+09	3.1581e+08
5.0e+06	1.1114e+04	1.4002e+04	2.3208e+04	1.8703e+09	4.5119e+08
6.5e+06	8.5496e+03	1.8202e+04	1.7852e+04	2.4314e+09	5.8654e+08
8.0e+06	6.9459e+03	2.2405e+04	1.4504e+04	2.9928e+09	7.2197e+08
9.5e+06	5.8506e+03	2.6599e+04	1.2217e+04	3.5531e+09	8.5712e+08
Models with $L_{xx} = 2.730\text{e+49}$					
5.0e+05	1.1116e+05	1.4001e+03	2.3246e+05	1.8618e+08	4.4936e+07
2.0e+06	2.7791e+04	5.6004e+03	5.8116e+04	7.4469e+08	1.7974e+08
3.5e+06	1.5881e+04	9.8003e+03	3.3210e+04	1.3032e+09	3.1453e+08
5.0e+06	1.1116e+04	1.4001e+04	2.3246e+04	1.8617e+09	4.4935e+08
6.5e+06	8.5515e+03	1.8200e+04	1.7883e+04	2.4201e+09	5.8412e+08
8.0e+06	6.9477e+03	2.2401e+04	1.4529e+04	2.9787e+09	7.1895e+08
9.5e+06	5.8506e+03	2.6602e+04	1.2235e+04	3.5373e+09	8.5377e+08

Table 13. Case  $M/M_\odot = 1.32$ : Results concerning the perpendicular rotator (part I)

$L_{xx}$	$P_{RR}$	$T_{RR}$	$I_{11}$	$I_{33}$	$\langle H_{ts} \rangle$	$H_{t[\max]}$	$\langle H_t \rangle$	$\omega_e^{-1}$
1.450e+49	14.8896	3.0594e+48	3.4362e+49	3.1499e+49	1.1025e+09	8.3213e+12	2.7960e+12	1.0000
1.500e+49	14.4496	3.2613e+48	3.4496e+49	3.1499e+49	1.1025e+09	8.3213e+12	2.7960e+12	1.0000
1.800e+49	12.3443	4.5810e+48	3.5364e+49	3.1499e+49	1.1025e+09	8.3213e+12	2.7960e+12	1.0000
2.100e+49	10.8524	6.0792e+48	3.6271e+49	3.1499e+49	1.1025e+09	8.3213e+12	2.7960e+12	1.0000
2.400e+49	9.7603	7.7250e+48	3.7282e+49	3.1499e+49	1.1025e+09	8.3213e+12	2.7960e+12	1.0000
2.700e+49	8.9148	9.5149e+48	3.8309e+49	3.1499e+49	1.1025e+09	8.3213e+12	2.7960e+12	1.0000
2.730e+49	8.8410	9.7009e+48	3.8413e+49	3.1499e+49	1.1025e+09	8.3213e+12	2.7960e+12	1.0000

Table 14. Case  $M/M_{\odot} = 1.32$ : Results concerning the perpendicular rotator (part II)

$B_s$	$\beta_*^p$	$V_{As}$	$t_{As}$	$H_p[\max]$	$\langle H_p \rangle$
Models with $L_{xx} = 1.450e+49$					
5.3e+05	1.0358e+05	1.4914e+03	1.9978e+05	2.5468e+08	5.9781e+07
2.1e+06	2.5894e+04	5.9654e+03	4.9945e+04	1.0187e+09	2.3912e+08
3.7e+06	1.4797e+04	1.0439e+04	2.8541e+04	1.7827e+09	4.1844e+08
5.3e+06	1.0357e+04	1.4915e+04	1.9977e+04	2.5470e+09	5.9784e+08
6.9e+06	7.9670e+03	1.9389e+04	1.5367e+04	3.3110e+09	7.7718e+08
8.5e+06	6.4736e+03	2.3862e+04	1.2486e+04	4.0748e+09	9.5648e+08
1.0e+07	5.4512e+03	2.8337e+04	1.0515e+04	4.8390e+09	1.1359e+09
Models with $L_{xx} = 1.500e+49$					
5.3e+05	1.0314e+05	1.4976e+03	1.9895e+05	2.5575e+08	6.0031e+07
2.1e+06	2.5785e+04	5.9906e+03	4.9736e+04	1.0230e+09	2.4013e+08
3.7e+06	1.4734e+04	1.0484e+04	2.8420e+04	1.7903e+09	4.2023e+08
5.3e+06	1.0315e+04	1.4975e+04	1.9896e+04	2.5573e+09	6.0028e+08
7.0e+06	7.9346e+03	1.9468e+04	1.5304e+04	3.3245e+09	7.8036e+08
8.6e+06	6.4469e+03	2.3960e+04	1.2435e+04	4.0917e+09	9.6044e+08
1.0e+07	5.4284e+03	2.8456e+04	1.0470e+04	4.8594e+09	1.1406e+09
Models with $L_{xx} = 1.800e+49$					
5.5e+05	1.0041e+05	1.5384e+03	1.9367e+05	2.6271e+08	6.1666e+07
2.2e+06	2.5103e+04	6.1535e+03	4.8419e+04	1.0508e+09	2.4666e+08
3.8e+06	1.4343e+04	1.0770e+04	2.7666e+04	1.8391e+09	4.3169e+08
5.5e+06	1.0040e+04	1.5385e+04	1.9366e+04	2.6273e+09	6.1670e+08
7.1e+06	7.7229e+03	2.0002e+04	1.4896e+04	3.4157e+09	8.0175e+08
8.8e+06	6.2752e+03	2.4616e+04	1.2104e+04	4.2036e+09	9.8671e+08
1.0e+07	5.2853e+03	2.9226e+04	1.0194e+04	4.9910e+09	1.1715e+09
Models with $L_{xx} = 2.100e+49$					
5.7e+05	9.7465e+04	1.5849e+03	1.8799e+05	2.7065e+08	6.3528e+07
2.3e+06	2.4366e+04	6.3395e+03	4.6999e+04	1.0826e+09	2.5411e+08
4.0e+06	1.3924e+04	1.1094e+04	2.6856e+04	1.8945e+09	4.4470e+08
5.7e+06	9.7466e+03	1.5849e+04	1.8799e+04	2.7065e+09	6.3528e+08
7.4e+06	7.4978e+03	2.0602e+04	1.4462e+04	3.5182e+09	8.2582e+08
9.1e+06	6.0921e+03	2.5356e+04	1.1751e+04	4.3300e+09	1.0164e+09
1.1e+07	5.1289e+03	3.0118e+04	9.8928e+03	5.1432e+09	1.2072e+09
Models with $L_{xx} = 2.400e+49$					
5.8e+05	9.4339e+04	1.6374e+03	1.8196e+05	2.7962e+08	6.5634e+07
2.3e+06	2.3584e+04	6.5497e+03	4.5490e+04	1.1185e+09	2.6254e+08
4.1e+06	1.3477e+04	1.1461e+04	2.5996e+04	1.9573e+09	4.5942e+08
5.8e+06	9.4338e+03	1.6374e+04	1.8196e+04	2.7962e+09	6.5635e+08
7.6e+06	7.2575e+03	2.1284e+04	1.3998e+04	3.6347e+09	8.5316e+08

Table 14—Continued

$B_s$	$\beta_*^p$	$V_{As}$	$t_{As}$	$H_p[\max]$	$\langle H_p \rangle$
9.4e+06	5.8957e+03	2.6201e+04	1.1372e+04	4.4743e+09	1.0502e+09
1.1e+07	4.9649e+03	3.1113e+04	9.5764e+03	5.3131e+09	1.2471e+09
Models with $L_{xx} = 2.700\text{e+49}$					
6.1e+05	9.1131e+04	1.6950e+03	1.7578e+05	2.8946e+08	6.7944e+07
2.4e+06	2.2783e+04	6.7800e+03	4.3945e+04	1.1578e+09	2.7177e+08
4.2e+06	1.3020e+04	1.1864e+04	2.5113e+04	2.0261e+09	4.7558e+08
6.1e+06	9.1133e+03	1.6950e+04	1.7578e+04	2.8945e+09	6.7942e+08
7.9e+06	7.0095e+03	2.2037e+04	1.3520e+04	3.7633e+09	8.8334e+08
9.7e+06	5.6954e+03	2.7122e+04	1.0985e+04	4.6316e+09	1.0872e+09
1.1e+07	4.7970e+03	3.2201e+04	9.2526e+03	5.4990e+09	1.2908e+09
Models with $L_{xx} = 2.730\text{e+49}$					
6.1e+05	9.0809e+04	1.7010e+03	1.7515e+05	2.9049e+08	6.8185e+07
2.4e+06	2.2701e+04	6.8045e+03	4.3787e+04	1.1620e+09	2.7275e+08
4.3e+06	1.2972e+04	1.1908e+04	2.5021e+04	2.0335e+09	4.7733e+08
6.1e+06	9.0809e+03	1.7010e+04	1.7516e+04	2.9049e+09	6.8185e+08
7.9e+06	6.9848e+03	2.2115e+04	1.3472e+04	3.7766e+09	8.8648e+08
9.7e+06	5.6763e+03	2.7213e+04	1.0949e+04	4.6472e+09	1.0908e+09
1.2e+07	4.7799e+03	3.2317e+04	9.2195e+03	5.5187e+09	1.2954e+09

Table 15. Case  $M/M_{\odot} = 1.32$ : Results concerning the turn-over phase

$B_s$	$f$	$t_{\text{TOV}}$	$\dot{P}_{\text{TOV}}$	$N_{xx}$	$t_{\text{now}}$	$\dot{T}$
$L_{xx} = 1.450\text{e+49}, A_r = 1.0630, \chi_{\text{now}} = 2.6088, F_{r[\text{now}]} = 0.9993$						
5.0e+05	5.0033e+22	5.1102e+09	4.2833e-17	2.0178e+16	9.7247e+06	2.2362e+30
2.0e+06	2.0013e+23	2.9030e+08	7.5400e-16	1.1462e+15	5.5243e+05	3.9365e+31
3.5e+06	3.5023e+23	1.0109e+08	2.1652e-15	3.9917e+14	1.9238e+05	1.1304e+32
5.0e+06	5.0033e+23	5.1160e+07	4.2785e-15	2.0200e+14	9.7356e+04	2.2337e+32
6.5e+06	6.5043e+23	3.0327e+07	7.2174e-15	1.1975e+14	5.7712e+04	3.7681e+32
8.0e+06	8.0053e+23	1.9320e+07	1.1329e-14	7.6285e+13	3.6766e+04	5.9149e+32
9.5e+06	9.5063e+23	1.3724e+07	1.5949e-14	5.4189e+13	2.6117e+04	8.3267e+32
$L_{xx} = 1.500\text{e+49}, A_r = 1.0672, \chi_{\text{now}} = 10.5276, F_{r[\text{now}]} = 0.9835$						
5.0e+05	5.0243e+22	4.4365e+09	4.7799e-17	1.8025e+16	1.5783e+08	2.7093e+30
2.0e+06	2.0097e+23	2.5201e+08	8.4148e-16	1.0239e+15	8.9652e+06	4.7696e+31
3.5e+06	3.5170e+23	8.7777e+07	2.4159e-15	3.5662e+14	3.1226e+06	1.3694e+32
5.0e+06	5.0243e+23	4.4414e+07	4.7746e-15	1.8045e+14	1.5800e+06	2.7063e+32
6.5e+06	6.5316e+23	2.6320e+07	8.0571e-15	1.0693e+14	9.3632e+05	4.5669e+32
8.0e+06	8.0388e+23	1.6776e+07	1.2641e-14	6.8157e+13	5.9680e+05	7.1650e+32
9.5e+06	9.5461e+23	1.1911e+07	1.7804e-14	4.8390e+13	4.2372e+05	1.0092e+33
$L_{xx} = 1.800\text{e+49}, A_r = 1.0940, \chi_{\text{now}} = 45.5260, F_{r[\text{now}]} = 0.7008$						
5.0e+05	5.1611e+22	2.0819e+09	8.5756e-17	9.7791e+15	4.7557e+08	7.3889e+30
2.0e+06	2.0645e+23	1.1827e+08	1.5096e-15	5.5552e+14	2.7015e+07	1.3007e+32
3.5e+06	3.6128e+23	4.1189e+07	4.3346e-15	1.9347e+14	9.4086e+06	3.7348e+32
5.0e+06	5.1611e+23	2.0846e+07	8.5646e-15	9.7917e+13	4.7618e+06	7.3794e+32
6.5e+06	6.7095e+23	1.2351e+07	1.4455e-14	5.8014e+13	2.8213e+06	1.2455e+33
8.0e+06	8.2578e+23	7.8719e+06	2.2681e-14	3.6975e+13	1.7981e+06	1.9542e+33
9.5e+06	9.8062e+23	5.5914e+06	3.1931e-14	2.6264e+13	1.2772e+06	2.7512e+33
$L_{xx} = 2.100\text{e+49}, A_r = 1.1221, \chi_{\text{now}} = 78.1579, F_{r[\text{now}]} = 0.2053$						
5.0e+05	5.3169e+22	1.0344e+09	1.4928e-16	5.4526e+15	4.2851e+08	1.7137e+31
2.0e+06	2.1268e+23	5.8767e+07	2.6276e-15	3.0977e+14	2.4344e+07	3.0165e+32
3.5e+06	3.7219e+23	2.0466e+07	7.5448e-15	1.0788e+14	8.4782e+06	8.6615e+32
5.0e+06	5.3169e+23	1.0355e+07	1.4913e-14	5.4581e+13	4.2894e+06	1.7120e+33
6.5e+06	6.9120e+23	6.1359e+06	2.5166e-14	3.2343e+13	2.5418e+06	2.8891e+33
8.0e+06	8.5071e+23	3.9104e+06	3.9488e-14	2.0612e+13	1.6199e+06	4.5333e+33
9.5e+06	1.0102e+24	2.7771e+06	5.5603e-14	1.4638e+13	1.1504e+06	6.3833e+33
$L_{xx} = 2.400\text{e+49}, A_r = 1.1534, \chi_{\text{now}} = 88.1526, F_{r[\text{now}]} = 0.0322$						
5.0e+05	5.4929e+22	5.4496e+08	2.5042e-16	3.1495e+15	3.2205e+08	3.4448e+31
2.0e+06	2.1972e+23	3.0965e+07	4.4072e-15	1.7896e+14	1.8300e+07	6.0626e+32
3.5e+06	3.8450e+23	1.0782e+07	1.2657e-14	6.2315e+13	6.3721e+06	1.7411e+33
5.0e+06	5.4929e+23	5.4551e+06	2.5016e-14	3.1527e+13	3.2238e+06	3.4413e+33
6.5e+06	7.1407e+23	3.2334e+06	4.2207e-14	1.8687e+13	1.9108e+06	5.8060e+33

Table 15—Continued

$B_s$	$f$	$t_{\text{TOV}}$	$\dot{P}_{\text{TOV}}$	$N_{xx}$	$t_{\text{now}}$	$\dot{T}$
8.0e+06	8.7886e+23	2.0596e+06	6.6260e-14	1.1903e+13	1.2172e+06	9.1148e+33
9.5e+06	1.0436e+24	1.4634e+06	9.3258e-14	8.4572e+12	8.6480e+05	1.2829e+34
$L_{xx} = 2.700\text{e}+49, A_r = 1.1851, \chi_{\text{now}} = 89.7462, F_{r[\text{now}]} = 0.0044$						
5.0e+05	5.6865e+22	2.8011e+08	4.3328e-16	1.7363e+15	2.1316e+08	6.3199e+31
2.0e+06	2.2746e+23	1.5521e+07	7.8191e-15	9.6214e+13	1.1812e+07	1.1405e+33
3.5e+06	3.9806e+23	5.5422e+06	2.1898e-14	3.4355e+13	4.2175e+06	3.1942e+33
5.0e+06	5.6865e+23	2.8039e+06	4.3284e-14	1.7381e+13	2.1338e+06	6.3135e+33
6.5e+06	7.3925e+23	1.6616e+06	7.3040e-14	1.0300e+13	1.2645e+06	1.0654e+34
8.0e+06	9.0984e+23	1.0584e+06	1.1467e-13	6.5605e+12	8.0539e+05	1.6727e+34
9.5e+06	1.0804e+24	7.5232e+05	1.6132e-13	4.6635e+12	5.7250e+05	2.3531e+34
$L_{xx} = 2.730\text{e}+49, A_r = 1.1884, \chi_{\text{now}} = 89.7936, F_{r[\text{now}]} = 0.0036$						
5.0e+05	5.7068e+22	2.6103e+08	4.5968e-16	1.6279e+15	2.0302e+08	6.6925e+31
2.0e+06	2.2827e+23	1.4465e+07	8.2952e-15	9.0209e+13	1.1251e+07	1.2077e+33
3.5e+06	3.9947e+23	5.1648e+06	2.3233e-14	3.2209e+13	4.0170e+06	3.3824e+33
5.0e+06	5.7068e+23	2.6133e+06	4.5916e-14	1.6297e+13	2.0325e+06	6.6849e+33
6.5e+06	7.4188e+23	1.5488e+06	7.7475e-14	9.6587e+12	1.2046e+06	1.1279e+34
8.0e+06	9.1309e+23	9.8659e+05	1.2162e-13	6.1526e+12	7.6732e+05	1.7707e+34
9.5e+06	1.0843e+24	7.0094e+05	1.7119e-13	4.3712e+12	5.4516e+05	2.4923e+34